The Dynamics of Proton Transfer at the C Side of the Mitochondrial Membrane: Picosecond and Microsecond Measurements†

A. B. Kotlyar,* N. Borovok, S. Kiryati, E. Nachliel, and M. Gutman

Laser Laboratory for Fast Reactions in Biology, Department of Biochemistry, Tel Aviv University, Ramat Aviv 69978, Israel

Received June 29, 1993; Revised Manuscript Received November 8, 1993®

ABSTRACT: The excited-state proton emitter, pyranine (8-hydroxypyrene-1,3,6-trisulfonate), was introduced into the inner aqueous space of inside-out submitochondrial particles (SMP). Upon initiation of respiration, the dye recorded acidification of this space. Incorporation of high concentrations of the dye (~100 nmol/mg of protein) had no effect on the respiratory functions of the vesicles, nor on their capacity to execute $\Delta\mu H^+$-coupled reverse electron transfer. The respiratory control ratio (RCR) remained as high as RCR > 4. Pulse irradiation of the dye caused photodissociation of the proton from the 8-hydroxy position. The release of the proton and its reaction with the matrix of the inner space of SMP were monitored at two time intervals: nanosecond fluorimetry measured the dissociation of the proton from the excited dye molecule (ΦOH^*), while microsecond spectroscopy followed the reaction between the proton and the ground-state anion (ΦO^-). Numerical integration of the differential rate equations describes the diffusion of protons in the perturbed system. The nanosecond measurements yield the physical characteristics of the aqueous phase that dissolves the dye. The apparent dielectric constant of that space is rather low ($\epsilon = 20$). The diffusion coefficient of the proton is 2.3×10^{-5} cm^2/s, and the activity of water is $a_{H_2O} = 0.87$. All of these values imply that a large fraction of the intervesicular aqueous phase is taken up by the hydration layer of the lipids and proteins of the C side of the membrane. The microsecond dynamics measurements indicate that the rates of proton binding to the membrane surface components reach an equilibrium within 60 μs. On the basis of these figures, we conclude that, under physiological conditions, the inner space of submitochondrial vesicles is in a homogeneous state of protonation.

Energy transformations in mitochondria, chloroplasts, or bacterial membranes proceed through reversible proton fluxes. Exergonic enzyme systems, such as the mitochondrial respiratory chain, pump protons in a unidirectional mode across the membrane, building the electrochemical potential of proton gradient ($\Delta\mu H^+$). Other enzymes, such as ATPase or active transport carriers, are driven by the proton gradient and conserve energy by the formation of a product or uphill accumulation of solutes.

While the rate of $\Delta\mu H$ is undisputed, there is a basic misunderstanding of the dynamics of proton passage from the point of production by the respiratory chain to the site of consumption by ATPase. This lack of knowledge originates from basic experimental limitations. The accepted mode for generating protons on the surface of the mitochondrial membrane is by turning on the proton producing/consuming enzymes whose turnover times are much longer than the propagation of protons on a membrane. Thus, when experimental results are interpreted, there is no way to distinguish between events caused by peculiarities of the enzymes and those of the proton flux between the sites.

A method that can furnish information about proton flux is the laser-induced proton pulse (Gutman, 1984). Experimentally, it synchronizes a massive, transient phase of proton dissociation from aromatic alcohols and, by the appropriate time-resolved measurements, quantitates the reaction of the discharged proton with the environment. The analysis of the recorded transients is carried out by a precise, rigorous mathematical procedure. By this method, we calculated the second-order rate constants of the proton-transfer reaction, the diffusion coefficient of the proton, and the dielectric constant of the probed space (Shimoni et al., 1993a,b).

We applied this methodology (Gutman et al., 1993) to study the interaction between protons and the *M* side of the mitochondrial inner membrane. The observations, and corresponding analysis, revealed that the charges on the membrane's surface were clustered in domains large enough to establish their local rates of interaction with ions in the bulk solution The regions were interpreted as proteins embedded in acidic phospholipid membrane. We report here an investigation of the C side of the membrane, the face lining the inner space of submitochondrial particles. For that purpose, we first introduced the dye pyranine (8-hydroxypyrene-1,3,6-trisulfonate) into the aqueous inner phase of the submitochondrial vesicles. Subjection of the intravesicular dye to short intensive laser pulses synchronized a massive dissociation of the hydroxyl proton. The interaction of the protons, released in the vesicles, was monitored by time-resolved fluorimetry (with 50-ps resolution over a time frame of 20 ns) or absorbance changes (with 50-ns resolution over 200 μs of observation time). The observed signals were analyzed by numerical integration of differential rate equations (Gutman, 1984, 1986), and the physical parameters characterizing the intravesicular matrix were determined.

The fluorescence kinetics revealed that the aqueous phase has a low dielectric constant ($\epsilon_{app} = 20$), low diffusivity of protons ($D_H = 2.3 \times 10^{-5}$ cm^2/s), and low activity of water ($a_{H_2O} = 0.87$). These findings imply that the properties of the membrane's surface differ markedly from those of bulk water. The microsecond transient absorbance allowed us to monitor the rate of proton equilibration with intravesicular space. The time required for equilibration (~60 μs) is much shorter than the turnover time of the respiratory chain enzymes.

†This research is supported by the U. S. Navy Office of Naval Research (Grant No. N00014-89-J1622), the United States–Israel Binational Science Foundation (91-00226), and the Israeli Ministry of Science and Technology (3435291). A.B. is a Koret Foundation postdoctoral fellow.

® Abstract published in *Advance ACS Abstracts,* January 1, 1994.

0006-2960/94/0433-873$04.50/0

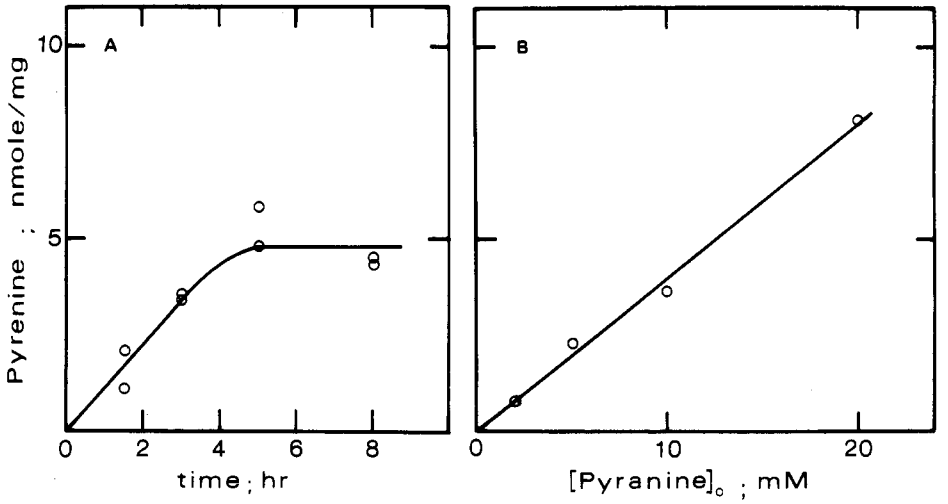

FIGURE 1: Accumulation of pyranine by submitochondrial particles. (A) SMP, at 10 mg/mL, were incubated with 10 mM dye at 0.25 M sucrose and 20 mM KCl (pH 9) at 30 °C. Samples were taken at intervals, and the amount of dye cochromatographed with the vesicles on a Sephadex G-50 column was determined. (B) SMP at 10 mg/mL were incubated for 3 h in the medium described above in the presence of varying dye concentrations. The vesicles were separated on a column and their dye content was measured.

The mechanism of propagation of protons within the submitochondrial space is discussed in detail, with special emphasis on the feasibility of proton confinement and the formation of a localized gradient. As it appears from our analysis, local gradients will have much shorter lifetimes than the catalytic activities of the system and, thus, cannot exist in physiologically functioning systems.

MATERIALS AND METHODS

Submitochondrial particles (SMP[1]) were prepared from heavy beef heart mitochondria as described by Racker and Horstman (1967). The respiratory control ratio, measured in the presence of a coupling concentration of oligomycin and NADH as substrate vs the rate in the presence of gramicidin, was RCR = 5 ± 0.7.

Incorporation of Pyranine. The incorporation of pyranine (8-hydroxypyrene-1,3,6-trisulfonate, ΦOH) was carried out by suspending SMP (at 10 mg/mL) in a solution containing 0.25 M sucrose, 20 mM KCl, and 10–20 mM pyranine (pH 9.0) at 30 °C for 3 h. The suspension was then passed over a 20 × 1 cm column of Sephadex G-50, preequilibrated with 250 mM sucrose and 20 mM KCl (pH 8.2). The passage was carried out at 4 °C at a flow rate of 20 mL/h. The nominal concentration of the dye collected with the vesicular fraction was 10–28 μM.

Quantitation of the Pyranine Concentration. Samples containing pyranine were diluted in 10 mM NaOH, and the dye concentration was measured, either spectrophotometrically (ϵ_{450nm} = 24 500 M^{-1} cm^{-1}) or fluorimetrically, against calibrated stock solutions.

Catalytic Activities. NADH oxidase, succinate oxidase, and reverse electron transport were measured as described previously (Gutman et al., 1993).

Time-resolved measurements of proton dissociation were carried out in two time domains. Microsecond kinetics was carried out using the third harmonic frequency of a Nd:YAG laser (355 nm, 1.8 mJ/pulse, ~1 MW/cm², 3 ns full-width at half-maximum, at a repetition rate of 10 Hz) for the excitation of the dye. The absorbance increment due to ΦO⁻ formation was measured at 457.8 nm using an argon laser. The transients were stored and averaged as previously described (Gutman et al., 1993).

Picosecond measurements were carried out using the time-correlated single photon counting system. Excitation pulses having a width of 1 ps at half-maximum and a wavelength of 300 nm were delivered at a frequency of 700 kHz, and the fluorescence was measured with a Hamamatzu R-3809 microchannel plate photomultiplier (Huppert et al., 1990).

The simulation of the measured dynamics was executed as previously described (Gutman, 1986; Yam et al., 1988) using a Silicon Graphics workstation.

Pyranine, laser grade, was purchased from Eastman Kodak. All other reagents were from Sigma Chemical Co.

RESULTS

Incorporation of Pyranine into Submitochondrial Vesicles. Pyranine is a highly charged molecule that cannot diffuse rapidly across pure phospholipid membranes (Clement & Gould, 1981; Gutman et al., 1989). On the other hand, exposure of submitochondrial vesicles to millimolar concentrations (2–20 mM) of pyranine (at 30 °C, pH 9) is accompanied by an appreciable penetration of the dye, detected as an increasing fraction of pyranine that cochromatographs with the vesicles (see Figure 1A). The amount of incorporation is proportional to the external concentration of the dye (frame B). Prolonged incubation of SMP with 20 mM pyranine dye had no effect on NADH oxidase and succinate oxidase activities, the sensitivity of respiration of rotenone or malonate, or the respiratory control ratio (RCR > 4) and the rate of reverse electron transport (driven by succinate oxidation).

The Intravesicular Location of the Dye. Addition of oxidizable substrate (NADH, succinate) to SMP loaded with pyranine causes rapid suppression of the fluorescence emission of the dye when irradiated at the wavelength of ΦO⁻ excitation (see Figure 2). When substrate is exhausted there is a slow recovery of ΦO⁻ concentration, which is accelerated by the addition of uncoupler. The acidification is not observed when respiration is blocked or when substrate is added after the uncoupler. On the basis of these observations, we conclude that the dye is located in a space that is accessible to protons generated during coupled respiration, but is inaccessible to the buffers in which the vesicles were suspended.

[1] Abbreviations: RCR, respiratory control ratio; SMP, submitochondrial particles; ΦOH and ΦO⁻, pyranine in its protonated and nonprotonated states, respectively; ΦOH* and ΦO*⁻, first electronically excited singlet state of pyranine in the corresponding states of protonation; HSA, human serum albumin.

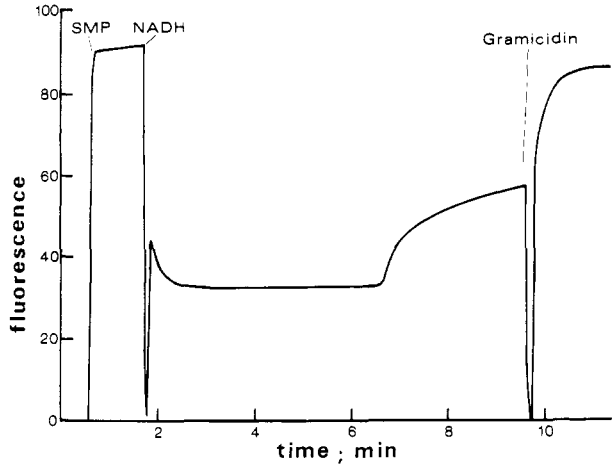

FIGURE 2: Acidification of pyranine in SMP during coupled oxidation of NADH. Submitochondrial vesicles containing pyranine were suspended (200 μg/mL) in a solution of 0.25 M sucrose, 20 mM KCl, 0.2 mM EDTA, and 2 mg/mL of human serum albumin (pH 8). The ground-state protonation of the dye was monitored fluorimetrically. The ground-state anion was selectively excited (λ_{ex} = 463 nm), and its emission (λ = 511 nm) was monitored continuously. At the times indicated on the chart, NADH (100 μM) and gramicidin were added. The incremental emission at ~6.5 min corresponds with the exhaustion of substrate.

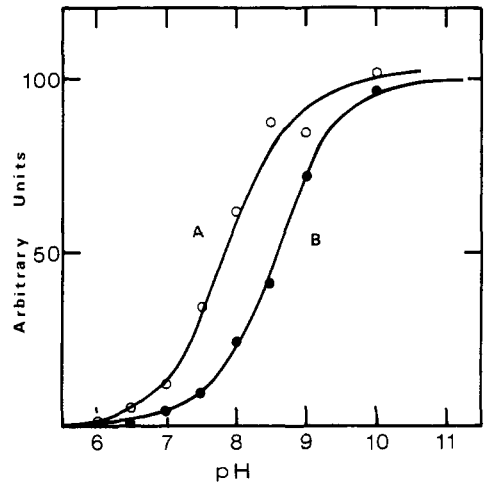

FIGURE 3: Effect of the absorption of pyranine to human serum albumin on its acid dissociation constant. The emission intensity of the dye (100 nM), excited selectively as ΦO^- (λ = 463 nm) and monitored at 511 nm, is drawn as function of pH. (A) The titration was carried out in 0.25 M sucrose and 20 mM KCl (○). (B) The titration was carried out in the same solution supplemented with 2 mg/mL HSA (●).

Leakage of Dye from the Vesicles. To monitor the efflux of the dye we exploited the capacity of serum albumin to form a stable complex with pyranine (Gutman, 1986). On binding to human serum albumin, the dye shifts its p*K* from 7.7 up to 8.6 (see Figure 3). When vesicles preloaded with dye are suspended at pH 8.0 in solution containing HSA, the leakage will appear as apparent quenching of the emission when excited at a wavelength where only ΦO^- is absorbing. Using that method, we followed the efflux of pyranine from SMP, and the results are shown in Figure 4. At 4 °C the efflux is a slow process, with $t_{1/2}$ ~ 3 h. At 30 °C the efflux is much faster and is not a single-exponential process.

On the basis of these observations, a standard procedure was defined. The vesicles were loaded with dye (20 mM, 3 h, 30 °C) and the suspension was cooled to 4 °C. Just before use, a small volume of suspension, containing vesicles in an amount sufficient for a single experiment, was passed through

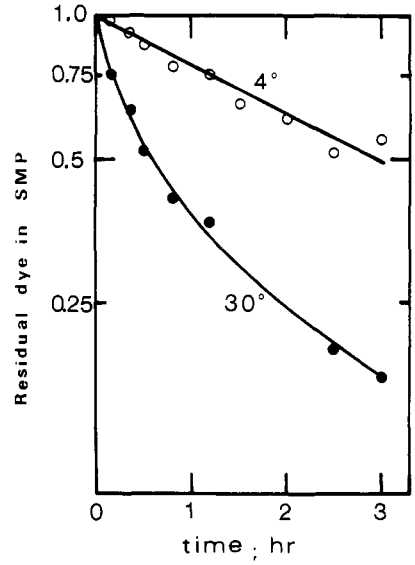

FIGURE 4: Dynamics of pyranine efflux from submitochondrial vesicles. The efflux was monitored as an apparent quenching of ΦO^- emission (λ_{ex} = 463 nm, λ = 511 nm). SMP preparation, loaded with dye, was suspended at 25–50 μg/mL in 0.25 M sucrose, 20 mM KCl, and 2 mg of HSA/mL (pH 8.0), and the emission at 511 nm was monitored at intervals. The ordinate denotes the fraction of dye remaining in the vesicular space, which is impermeable to HSA.

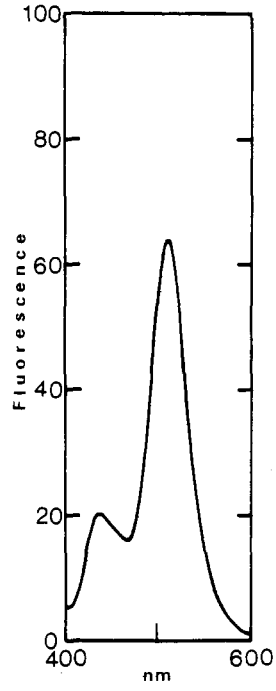

FIGURE 5: Fluorescence emission spectrum of pyranine enclosed in submitochondrial vesicles. The SMP, loaded with dye, were suspended (50 μg/mL) in 0.25 M sucrose and 20 mM KCl (pH 7.05) and uncoupled by 2 μg of gramicidin. The emission spectrum excitation wavelength (390 nm) was recorded within 5 min after emergence from the column.

a Sephadex column. The collected vesicles were immediately placed in an observation cell, and the laser irradiation experiments were initiated within 3–4 min after emergence from the column. Under these conditions, the fraction of the dye that leaked out was kept below ~4%.

Fluorescence of Pyranine in SMP. The emission spectrum of pyranine enclosed in submitochondrial vesicles is shown in Figure 5. The spectrum was measured at pH 7.05, where ~80% of the dye is in the ΦOH form, and the extinction coefficient of ΦO^-, at the excitation wavelength, is ~25% of

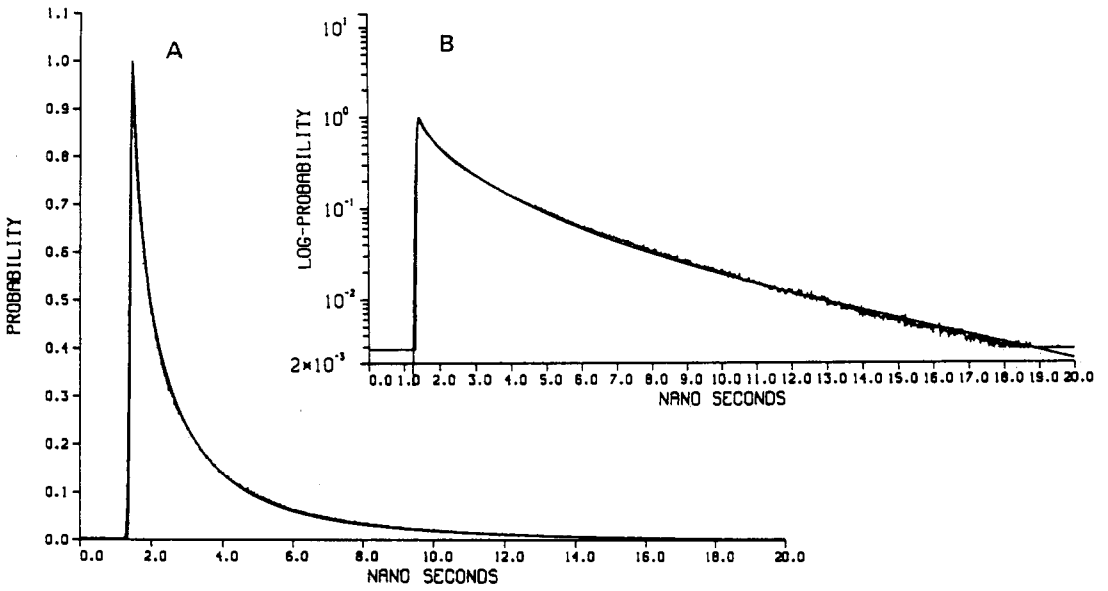

FIGURE 6: Time-resolved fluorescence of pyranine in submitochondrial particles. SMP, loaded with pyranine, were suspended in 0.25 M sucrose and 20 mM KCl (pH 8), and the fluorescence of ΦOH* was measured by time-correlated single photon counting techniques. Excitation (300 nm) and emission (435 nm) were recorded using a Hamamatsu R-3809 microchannel plate photomultiplier. For details see Pines et al. (1991). Both experimental results and theoretical reconstruction are drawn on a linear (frame A) and logarithmic (frame B) y axis. The fitting parameters are given in Table 1.

that of ΦOH. In spite of the fact that under such conditions the preferentially excited form is ΦOH, we find that the emission of ΦOH* (λ_{max} = 435 nm) is only 35% of the emission by ΦO^{*-} (λ_{max} = 515 nm). The reason for the enhanced ΦO^{*-} emission is the rapid dissociation of ΦOH* to the excited anion and solvated proton (Weller, 1961).

In pure water, the dissociation process is fast while the recombination of ΦO^{*-} with H^+ is inefficient; as a result, the steady-state ratio of the two forms is $I_{\Phi OH^*}/I_{\Phi O^{*-}} = 0.05$. As can be seen in Figure 5, in vesicles the ratio is much higher. The enhanced ratio implies that the immediate vicinity of the dye in the vesicles restricts the dissociation of the proton. It may be due to slower dissociation, faster recombination, or both. Elucidation of the dissociation mechanism can be obtained from time-resolved fluorescence of the excited molecule (Huppert et al., 1982). The time-resolved fluorescence measurements were carried out as described by Huppert et al. (1990), and the experimental tracings, together with the theoretical reconstruction of the dynamics (see Discussion), are shown in Figure 6. Frame A depicts the amplitude on a linear scale while frame B is drawn on a logarithmic scale. The fidelity of the reconstruction is high, and over a range of 3 orders of magnitude, the theoretical trace is within the envelope of the electronic or the statistical noise.

The reconstruction of the dynamics was achieved by the model of Agmon (Huppert et al., 1990) for translational diffusion of a proton within the electrostatic field of the pyranine anion (ΦO^{*-}), as it is modulated by the ionic strength of solution according to the Debye–Huckel equation (Pineset al., 1991). The various parameters are listed in Table 1 and will be discussed below.

Interaction of Protons with the Mitchondrial Membrane. Pyranine locked in the submitochondrial vesicles faces the C side of the membrane. When the dye dissociates, both ΦO^- and the discharged protons interact with the various proton-binding components of the membrane. In the short-time experiments (such as in Figure 6), the radius (r) of the space probed by the proton is approximated by $r = 2Dt$ = 100 Å, i.e., only the immediate vicinity of the fluorophore is probed by the proton.

Table 1: Physical and Kinetic Parameters Controlling the Dissociation of Protons from Excited Pyranine inside Submitochondrial Vesicles

parameter	SMP	bulk water
D_{H^+}[a]	2.3×10^{-5} cm²/s	9.3×10^{-5} cm²/s
ϵ[b]	20	80
k_f[c]	2.7×10^9 s^{-1}	7×10^9 s^{-1}
a_{H_2O}[d]	0.872	1.000
k_r[e]	5.5×10^9 Å/s	5.5×10^9 Å/s
k_{as}[f]	4×10^7 s^{-1}	
$(\Phi OH^*)_{(ud)}$[g]	8%	

[a] D_{H^+} is the diffusion coefficient of H^+. [b] ϵ is the dielectric constant of the reaction space. [c] k_f is the rate of proton dissociation for the excited molecule. [d] The activity of water as calculated from k_f according to Huppert et al. (1982). [e] k_r is the rate of proton recombination with ΦO^{*-} at the surface of the reaction sphere. [f] k_{as} is the rate of proton reaction with protonatable sites, such as carboxylates; see Table 2. [g] $(\Phi OH^*)_{(ud)}$ is the fraction of the ΦOH* population located in sites where it can not eject its proton due to a lack of water.

Another mode of the laser-induced proton pulse is to monitor the absorption of the ΦO^- anion formed upon relaxation of ΦO^{*-} (Gutman, 1984, 1986). In these experiments the dye is excited by a short laser pulse and the incremental absorption of ΦO^- is monitored (λ = 457.8 nm) in the microsecond time scale. The results of such measurements are given in Figure 7. The absorption of ΦO^- increases within the instrumental time and then relaxes over a period of 200 μs.

All reactions between the reactants present in the perturbed space (the pyranine, proton, and membranal buffering moieties) had been combined into a set of coupled, nonlinear parametric differential equations (Yam et al., 1988). The numerical integration of these equations with the parameters given in Table 2 reconstructed the observed signal and is depicted by the smooth curve in Figure 7.

DISCUSSION

The permeation of the dye across the mitochondrial membrane is orders of magnitude faster than its passage across a pure phospholipid membrane (Gutman et al., 1989). The leakage out of small unilamellar vesicles or multilamellar

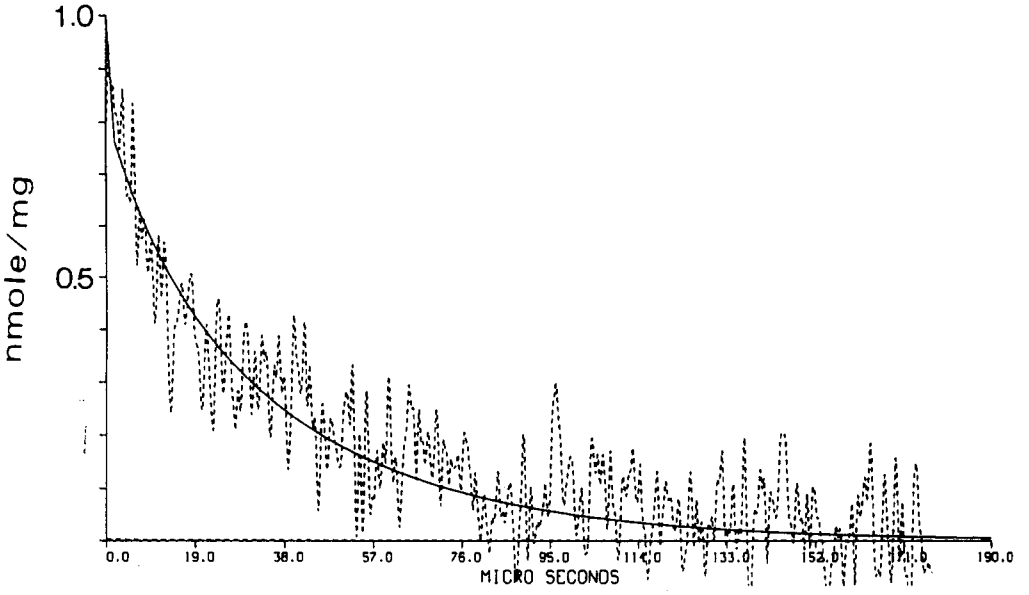

FIGURE 7: Time-resolved measurements of ΦO^- protonation in submitochondrial particles. SMP were labeled with pyranine at pH 7.4, passed over the column, and suspended at 4 mg/mL in 0.25 M sucrose, 20 mM KCl, and 2 mg of HSA/mL (pH 7.4). The suspension was probed by a continuous beam (λ = 457.9 nm) where only ΦO^- is absorbed and excited by a train (4096) of laser pulses (355 nm, 1.7 mJ/pulse) at a repetition rate of 10 Hz. The transient absorbance was amplified, digitized, and averaged. The continuous smooth line is a numerical reconstruction of the signal with the parameters listed in Table 2.

Table 2: Rate Constants and Reactant Concentrations Characterizing the Reaction of Protons inside Submitochondrial Vesicles

reactants	C	M
ΦOH	10 mM[a]	
pK (ΦOH)	7.7	7.7
RCOOH[b]	15	100 ± 10
pK (RCOOH)	5.0 ● 0.1	4.1
RNH_2	15	200 ± 20
pK (RNH_2)	6.7 ± 0.1	6.9
pH of experiment	7.4	6.0–8.7
ionic strength	70 mM	
rate constants[c]		
$\Phi O^- + H^+$	$(1.0 \pm 0.1) \times 10^{10}$	5×10^{10}
$RCOO^- + H^+$	$(0.3 \pm 0.2) \times 10^{10}$	7×10^{10}
$RNH_2 + H^+$	$(1.0 \pm 0.2) \times 10^{10}$	0.1×10^{10}
ΦO^- + RCOOH	$(1.0 \pm 0.2) \times 10^{7}$	5×10^{7}
$\Phi O^- + RNH_3^+$	$(3.0 \pm 0.2) \times 10^{6}$	4×10^{8}
RCOOH + RNH_2	$(1.0 \pm 0.5) \times 10^{6}$	3×10^{9}

[a] Internal concentration of dye is based on the inner space of 1 μL/mg of protein. [b] RCOOH and RNH_2 are quantitated in nmol/mg of protein. [c] All rate constants are given in units of M^{-1} s^{-1}.

vesicles is as low as 1% over a 24-h period. The plausible explanation is that in SMP the dye utilizes some of the mitochondrial physiological transport mechanism. That subject is still under investigation.

Incorporation of pyranine into SMP at millimolar concentrations had no effect on the catalytic activities of the respiratory chain, nor did it damage the energy conservation system of the membrane. Thus, the results presented above and the following discussion are pertinent to the chemical–physical properties of the native C surface of the mitochondrial membrane and the inner space of coupled, inside-out submitochondrial particles.

The pyranine, in our experiments, permeates at a moderate rate into the vesicles, occupies a space that is inaccessible to external buffer, and gauges the proton pumped by the respiratory activity. Consequently, the time-resolved proton dynamics, which we measured, are relevant to bioenergetics modeling just as are protons produced by the enzymic machinery.

The Intravesicular Location of the Dye. The sub-nanosecond dynamics, with their inherent limitation on the observation period, enables us to follow the proton as it probes the most immediate vicinity of the dye. The analytic formalism used for the reconstruction of the observed transients quantitates the dielectric constant, the proton's diffusion coefficient, and the water activity of the probed space.

The dielectric constant of the space probed by the proton is surprisingly low (see Table 1). The measured value, ϵ = 20, is lower than that measured for the aqueous interbilayer phase of multilamellar vesicles (Gutman et al., 1992). Such low values characterize the lipid–water interphase (Handa et al., 1990; Kimura & Ikegami, 1985), the surface lysozyme, or protein cavities (Yam et al., 1993; Gutman et al., 1992b; Shimoni et al., 1993a). Thus it appears that the dye is within a Debye length (for I = 80 mM, K^{-1} = 10 Å) from protein structures. The activity of water, which solvates the dye, is also compatible with that assignment (Yam et al., 1991; Shimoni et al., 1993a). The dissociation of ΦOH^* to ΦO^{*-} and H^+ requires that the medium is able to solvate the proton within a time frame of a few femtoseconds. In a case where the water molecules cannot rotate their dipole in the direction of the dissociating protonic charge, the stabilization of the proton will be insufficient, and the dissociation attempt will be aborted. For this reason the dissociation of ΦOH^* and other compounds is slowed in solutions of diminished water activity (Huppert et al., 1982). The slow rate of ΦOH^* dissociation in SMP corresponds with a water activity of a_{H_2O} = 0.87, which is consistent with the location of the dye within the hydration layer of the macromolecular structure, a region where the chemical potential of water is lower than that in the bulk solution (Gutman et al., 1982a,b; Bardez et al., 1984; Kreuer, 1992; Shimoni et al., 1993a,b).

The diffusion coefficient of protons in the probed space, D = 2.3×10^{-5} cm^2/s, is also compatible with an ordered environment. The diffusion of protons in water is controlled by the rate of water molecule rotatation to form a solvation shell. As the rate of rotation is slowed, so does the diffusion. Thus, the slow diffusivity of protons in SMP is also compatible

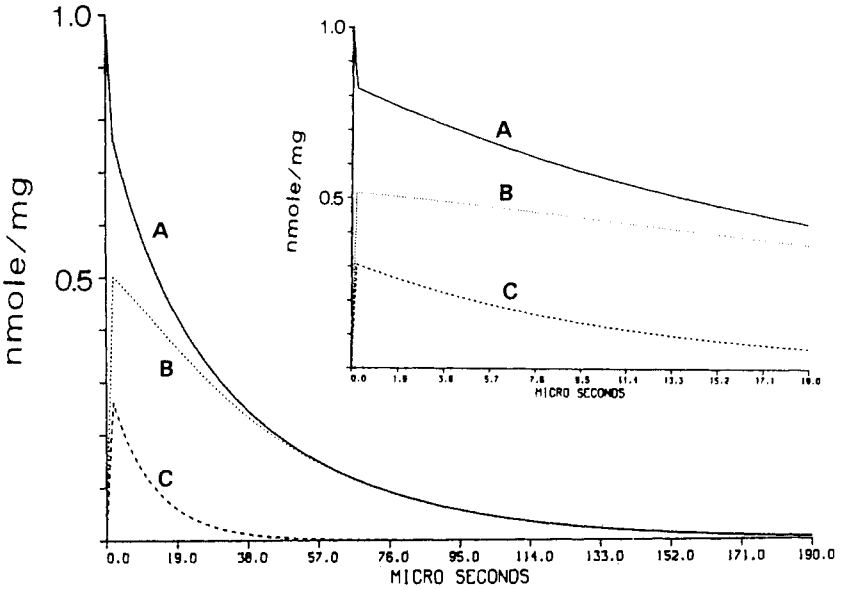

FIGURE 8: Simulation of the state of protonation of the C side components of the mitochondrial membrane. The curves drawn in the figure correspond with the reconstruction dynamics that mimic the events analyzed in Figure 7. Curve A depicts the protonation of ΦO^- in the bulk solution and is identical to that shown in Figure 7. Curve B depicts the protonation of the pK = 6.7 population (RNH_2), while curve C is for the carboxylates, pK = 5.0. The insert is an enlargement of the events during the first 20 μs.

with the location of the dye being close to a structure that interacts avidly with the water.

Finally, the simulation of nanosecond dynamics necessitates the inclusion of a discrete step of proton binding to some buffer moiety located in the dye's vicinity (k_{as} in Table 1). The rate of this reaction is comparable to that measured for a proton between phospholipid membranes (Gutman et al., 1992a).

All of the arguments discussed above indicate that the proton dissociation kinetics that we measured proceeds in the immediate vicinity or within the hydration layer of the components constituting the C face of the mitochondrial membrane. It is the same space to which the respiration-driven proton pumps discharge their protons.

Kinetics of the Proton Reaction with the C Side of the Mitochondrial Membrane. The microsecond dynamics, as in Figure 7, monitors the reaction of the proton with the pyranine anion and all other protonatable moieties present in the inner space. As no soluble buffer was present throughout the whole preparative work, we have to consider only the sessile buffers on the membrane.

In our previous work (Gutman et al., 1993), we demonstrated that the M side membrane can be approximated, for the sake of proton-binding kinetics, by two types of buffers. The carboxylates of the surface contribute a buffer capacity of 100 nmol/mg, while the histidine or low-pK amine moieties contribute twice that much (see Table 2). The C side membrane can be represented by the two types of buffer, but their quantities are much reduced and their pK values are somewhat different. These values are in accord with the fact that the mass of membranal proteins which protrude into the mitochondrial matrix is much larger than the mass of these protruding out of the C side.

The rates of proton binding to the C side are also different even in the order of magnitude from the reactivity of the M side components. The rate of protonation of the C side carboxylates is 20 times slower than the reaction of the M side components, and their pK is higher by almost 1 pK unit. Both findings are compatible with a reduced accessibility of the carboxylates and their confinement in a somewhat hydrophobic environment that thermodynamically favors the undissociated form. On the other hand, the medium pK buffer (RNH_2) of the C side exhibits higher reactivity than the M side.

The reactivity of the surface components with the pyranine anion is also nonidentical for the two faces of the membrane. The rate of proton exchange between ΦO^- and RNH_3^+ moieties on the C side is too slow to be diffusion-controlled. At present, further elaboration of these rate constants is avoided. Yet current experiments with reconstituted preparations may provide more information about the mechanism of protonation of the respiratory chain complexes.

Equilibration Time in SMP. The production of a proton on the C side surface is the physiological role of the redox-driven proton pumps. In our experiment we duplicated the event by photodissociation of the dye. Thus, by simulating the state of protonation of all components as a function of time, we can gain some insight into the fate of a proton injected into the inner space of SMP during its physiological function. This scenario is illustrated in Figure 8. The uppermost curve (A) is the state of protonation of ΦO^-, as shown in the fitted curve in Figure 7. Curves B and C depict the protonation of the pK = 6.7 and pK = 5 buffering components respectively.

During the initial phase of the perturbation (see insert to Figure 8), the state of protonation is controlled by kinetics. The incremental protonation is not a function of the pK but of the rate constant. The pK = 6.7 buffer (B) picks about twice as many protons as the other buffer, while at equilibrium their ratio should be about a ~50-fold excess. That state of disequilibrium is very brief. Within a few microseconds, the proton distribution readjusts and drifts toward equilibrium. The excessive protonation of RCOOH relaxes rapidly, while that of RNH_2 enjoys a longer lifetime. At about 60 μs the proton had been reshuffled. The carboxylates are reionized, the high-pK moieties retain the protons, and curves B (extra protonation of RNH_2) and A (proton missing from ΦOH) overlap. At that stage, the surface components are in equilibrium among themselves, while the bulk–surface system is still in disequilibrium, as evident by the excessive protonation of the membrane component. The progression of the reaction from that time point onward is the equlibration between bulk and surface which lasts ~200 μs.

What is evident from these figures is that in a perturbed multiequilibrated system the relaxation is not homogeneous and some systems respond faster than others. For the C side of the mitochondrial membrane, the membranal components reach equilibrium in ~60 μs, and bulk–surface equilibrium is established in about twice that time. These time constants are significantly shorter than the turnover time of energy-coupled proton pumps (~1 ms). In other words, the kinetic parameters of the submitochondrial membrane are such that a state of local disequilibrium (localized proton gradient) cannot exist under physiological conditions.

REFERENCES

Bardez, E., Goguillon, B. T., Keh, E., & Valeur, B. (1984) *J. Phys. Chem. 88*, 1909–1913.

Clement, N. R., & Gould, J. M. (1981) *Biochemistry 20*, 1534–1538.

Gutman, M. (1984) *Methods Biochem. Anal. 30*, 1–103.

Gutman, M. (1986) *Methods Enzymol. 127*, 522–538.

Gutman, M., Huppert, D., & Nachliel, E. (1982a) *Eur. J. Biochem. 121*, 637–642.

Gutman, M., Nachliel, E., & Huppert, D. (1982b) *Eur. J. Biochem. 125*, 175–181.

Gutman, M., Nachliel, E., & Moshiach, S. (1989) *Biochemistry 28*, 2936–2940.

Gutman, M., Nachliel, E., & Kiryati, S. (1992a) *Biophys. J. 63*, 281–290.

Gutman, M., Tsfadia, Y., Masad, A., & Nachliel, E. (1992b) *Biochim. Biophys. Acta 1109*, 141–148.

Gutman, M., Kotlyar, A. B., Borovok, N., & Nachliel, E. (1993) *Biochemistry 32*, 2942–2946.

Handa, T., Kakagaki, M., & Miyajima, K. (1990) *J. Colloid Interface Sci. 137*, 253–262.

Huppert, D., Kolodney, E., Gutman, M., & Nachliel, E. (1982) *J. Am. Chem. Soc. 104*, 6949–6953.

Huppert, D., Pines, E., & Agmon, N. (1990) *J. Opt. Soc. Am. B 7*, 1545–1550.

Kimura, Y., & Ikegami, A. (1985) *J. Membr. Biol. 85*, 225–231.

Kreuer, R.-D. (1992) in *Proton Conductors—Solids, membranes and gels—materials and devices* (Colomban, P., Ed.) p 474, Cambridge University Press, Cambridge, UK.

Pines, E., Huppert, D., & Agmon, M. (1991) *J. Phys. Chem. 95*, 666–674.

Racker, E., & Horstman, L. (1967) *J. Biol. Chem. 242*, 2547–2556.

Shimoni, E., Tsfadia, Y., Nachliel, E., & Gutman, M. (1993a) *Biochem. J. 64*, 472–479.

Shimoni, E., Nachliel, E., & Gutman, M. (1993b) *Biophys. J. 63*, 480–483.

Weller, A. (1961) *Prog. React. Kinet. 1*, 189–214.

Yam R., Nachliel, E., & Gutman, M. (1988) *J. Am. Chem. Soc. 110*, 2636–2640.

Yam, R., Nachliel, E., Kiryati, S., Gutman, M., & Huppert, D. (1991) *Biophys. J. 59*, 4–11.